Model Free Barrier Functions via Implicit Evading Maneuvers

Eric Squires[1]

Georgia Tech Research Institute

Rohit Konda

UC Santa Barbara

Samuel Coogan

Georgia Institute of Technology

Magnus Egerstedt

UC Irvine

Abstract

This paper demonstrates that in some cases the safety override arising from the use of a barrier function can be needlessly restrictive. In particular, we examine the case of fixed wing collision avoidance and show that when using a barrier function, there are cases where two fixed wing aircraft can come closer to colliding than if there were no barrier function at all. In addition, we construct cases where the barrier function labels the system as unsafe even when the vehicles start arbitrarily far apart. In other words, the barrier function ensures safety but with unnecessary costs to performance. We therefore introduce model free barrier functions which take a data driven approach to creating a barrier function. We demonstrate the effectiveness of model free barrier functions in a collision avoidance simulation of two fixed-wing aircraft.

[1]Corresponding author, `eric.squires@gtri.gatech.edu`

1. INTRODUCTION

Barrier functions [1], a function of the state whose derivative is bounded, can be used to maximize the performance of a system while satisfying a safety constraint. However, if the safety constraint arising from the barrier function is overly restrictive then performance can be needlessly diminished. For example, in an adaptive cruise control setting, safety designers can choose a minimum inter-vehicle distance that the vehicle must satisfy. Setting this minimum distance too high (e.g., hundreds of meters) will result in excessive inter-vehicle distances where speed setpoints are difficult to achieve. In other words, the performance goal (speed) is negatively impacted by an overly conservative constraint (inter-vehicle distances).

In this paper we generalize this point by demonstrating that it extends beyond simple scalar settings like inter-vehicle distance. In particular, we consider the case of unmanned aerial vehicle (UAV) collision avoidance and demonstrate that even with a fixed minimum inter-vehicle safety distance, the observed behavior of the safety override resulting from a barrier function can be needlessly conservative. Specifically, we first consider the case where the barrier function safety constraint ensures each vehicle can maintain a straight trajectory without a future collision. We show in this case that even when the vehicles are arbitrarily far apart that the barrier function indicates the vehicles are unsafe. This can result in significant performance implications on a waypoint-following UAV. To see this, consider another vehicle located far away and its effect on how well our own vehicle achieves its waypoints. The other vehicle could orient itself in a way that makes the barrier function imply an override is needed. This can make the system more unpredictable as non-local factors (e.g., vehicles far away) can have significant impact on the control choices. Further, it could even be exploited by malevolent actors who could conceivably choose to orient their own aircraft in a way that forces the waypoint-following aircraft to adjust and move in a way that a malevolent actor intends.

However, the concerns go further than that. We therefore consider a second case where a barrier function ensures the vehicles can employ a turning maneuver to maintain safe distances for all future time. However, in this case we construct a scenario where the nominal controller, a controller designed for a performance objective like waypoint following but that does not ensure safety, would result in inter-vehicle distances many times greater than the minimum safety threshold. Nevertheless, when an override from a barrier function is employed, the vehicles significantly alter their course in a way that causes them to barely exceed the minimum safety distance from each other. In other words, not only does the safety override needlessly alter the original system's control value, significantly reducing system performance, in doing so it also causes the vehicles to barely exceed the safety thresholds. Further, it can reduce trust in a system as observers see the safety override causing the system to fly needlessly close to the other vehicle.

Prior work has investigated how to relax the invasiveness of an override while ensuring that the system is always safe, often looking at how to construct a barrier function that specifically accounts for the nominal controller. For instance, in [2] the authors introduce an optimization to maximize the set of safe states that are compatible with a region of attraction so that the safety constraint considers the performance objective. Similarly, a nominal controller and barrier function are learned simultaneously in [3]. Imitation learning has also been employed as in [4] where a barrier function is constructed from expert trajectories where the expert is able to consider both performance and safety factors. More broadly, barrier functions have also been used to not only enforce safety constraints but also guide exploration in [5] via off policy reinforcement learning. Similarly, in [6] the authors introduce a barrier function to constrain the policy update in reinforcement learning.

In this paper, rather than simultaneously training both the nominal controller and safety override, we instead seek to maximize the set of safe controls available that could be applied to any nominal policy. This allows for a separation of concerns that simplifies the controller design process [7]– the nominal controller can be designed for performance while the safety override resulting from the barrier function overrides the nominal controller as little as possible while improving safety. In particular, we show that maximizing the set of safe states is not enough to ensure that a safety override is not restrictive. In other words, given a state that is safe for two different barrier functions, it may be that the available set of controls to keep the system safe is larger for a barrier function that has a smaller overall safe set.

We also construct a barrier function without requiring a dynamics model. A benefit of this is that it reduces the model mismatch that can occur when using simplified modeling assumptions (e.g., assuming linearity in the control input even though aircraft are subject to 6-DOF dynamics) that can lead to differences in simulated versus real-world performance. It has been more broadly discussed that model-free approaches can often outperform model-based systems [8] as they are less restricted in fitting to data. Thus, we propose model free barrier functions, which are learned from interactions with the environment, to reduce how much the system is overridden. This paper makes the following contributions. First, we motivate model free barrier functions with examples from fixed wing collision avoidance [9] that demonstrates a model based approach induces unnecessary overrides. Second, we derive model free barrier functions. Third, we demonstrate the approach in simulation. A video of the behavior is also available [10].

This paper is organized as follows. Section 2 introduces the background for barrier functions. Section 3 derives model free barrier functions. Section 4 demonstrates the algorithm in simulation.

2. Background

In this paper we compare model based and model free barrier functions with the example of UAV collision avoidance. Thus we introduce a UAV dynamics model for two UAVs indexed by i ($i \in \{1, 2\}$) where the state for each UAV at time k is given by $x_{k,i} = \begin{bmatrix} p_{k,i,x} & p_{k,i,y} & \theta_{k,i} & p_{k,i,z} \end{bmatrix}^T$. The components $p_{k,i,x}$, $p_{k,i,y}$, and $p_{k,i,z}$ are the x, y, and z position of aircraft i and $\theta_{k,i}$ is the orientation. The discrete time dynamics are given by

$$x_{k+1,i} = \begin{bmatrix} p_{k,i,x} + v_{k,i} \cos \theta_{k,i} \Delta t \\ p_{k,i,y} + v_{k,i} \sin \theta_{k,i} \Delta t \\ \omega_{k,i} \Delta t \\ p_{k,i,z} + \zeta_{k,i} \Delta t \end{bmatrix}$$

where $v_{k,i}$ is the translational velocity, $\omega_{k,i}$ is the rotational velocity, $\zeta_{k,i}$ is the vertical velocity, and Δt is a integration step parameter. These velocities serve as control inputs and are subject to actuator limits v_{min} and v_{max} where $v_{min} > 0$, $|\omega_{k,i}| \leq \omega_{max}$, and $|\zeta| < \zeta_{max}$, respectively. Given two aircraft, the system with state $x_k = \begin{bmatrix} x_{k,1}^T & x_{k,2}^T \end{bmatrix}^T$ has dynamics of the form

$$x_{k+1} = f(x_k, u_k) \tag{1}$$

where $x_k \in \mathbb{R}^n$, $u_k \in U \subset \mathbb{R}^m$, and U is the set of available controls for the system. In [11] the authors consider dynamics of the form (1) to develop barrier functions for discrete time systems which we briefly summarize here. Let $h : \mathbb{R}^n \to \mathbb{R}$ be an output function of the state and define the safe set $\mathcal{C}$ as a superlevel set of h so that

$$\mathcal{C} = \{x_k \in \mathbb{R}^n \ : \ h(x_k) \geq 0\}. \tag{2}$$

We also let $\Delta h(x_k, u_k) = h(x_{k+1}) - h(x_k)$. When the output function h satisfies the following property it can be used to ensure that if the state starts in $\mathcal{C}$ then it will stay in $\mathcal{C}$ for all future time. The following definition is an adaptation from Definition 4 of [11] using terminology similar to that in [1].

Definition 1. A map $h : \mathbb{R}^n \to \mathbb{R}$ is a *Discrete-Time Exponential Control Barrier Function (DT-ECBF)* on a set $\mathcal{D}$ where $\mathcal{C} \subseteq \mathcal{D}$ if there exists a control input $u_k \in \mathbb{R}^m$ and λ such that

$$\Delta h(x, u) + \lambda h(x) \geq 0 \tag{3}$$

and $0 \leq \lambda \leq 1$ for all $x \in \mathcal{D}$.

We therefore define the admissible control space as

$$K(x_k) = \{u \in U \, : \, \Delta h(x_k, u_k) + \lambda h(x_k) \geq 0\}. \tag{4}$$

The following is an adaptation from Proposition 4 of [11] using the terminology of an admissible control space from [1].

Proposition 1. *Given a set $\mathcal{C} \subset \mathbb{R}^n$ defined in (2) for an output function h, if h is a DT-ECBF on $\mathcal{D}$ then any controller $u : \mathbb{R}^n \to U$ such that $u(x) \in K(x)$ for all $x \in D$ will render the set $\mathcal{C}$ forward invariant.*

Assuming the system has a nominal controller designed to achieve a performance goal that does not necessarily ensure safety, barrier functions can be used to select a control value u as close as possible to the original controller $\hat{u}$ while ensuring safety via the following optimization program:

$$\begin{aligned} u = \arg\min_{u \in U} & \ \frac{1}{2} \|u - \hat{u}\|^2 \\ \text{s.t.} \quad & u \in U \\ & u \in K(x). \end{aligned} \tag{5}$$

As discussed in [11], equation (5) is a nonconvex program which can be difficult to solve in real-time. We resolve this runtime issue in this paper by assuming U is a discrete set small enough to calculate this optimization in real time. The final implementation is in a neural network where a single forward pass through a network can calculate many values for $K(x)$ in parallel as discussed for instance in [12].

3. Generating a Model Free Barrier Function via Evasive Maneuvers

3.1. Constructing Barrier Functions For Discrete Time Systems

In [9] the authors demonstrate a method for constructing a barrier function for continuous time systems. We therefore first adapt the method shown in that paper to discrete time. Note that a similar approach is introduced in [13] although [9] does not require a backup set. Let $\rho : \mathbb{R}^n \to \mathbb{R}$ be a safety function that must be nonnegative at all times for the system to be safe. Let $\gamma : \mathbb{R}^n \to U$ be an evasive maneuver that can keep the system safe. Note that γ is not necessarily the safety override but is instead used to construct a barrier function. To construct a candidate DT-ECBF we forward propagate the state using γ as the controller and calculate the worst case safety value using ρ for all future times. In other words, let

$$h(x_0) = \inf_{k \geq 0} \rho(\hat{x}_k) \tag{6}$$

be a candidate DT-ECBF where $\hat{x}_0 = x_0$ and $\hat{x}_k$ for $k > 0$ is the future state when using γ for all future time, namely

$$\hat{x}_{k+1} = f(\hat{x}_k, \gamma(\hat{x}_k)). \tag{7}$$

Using this formulation, we can show that h in (6) is a DT-ECBF. The theorem and proof are similar to Theorem 2 of [9] but applied to discrete time systems.

Theorem 1. *Given a dynamical system (1) and a function h defined in (6) with a safety function ρ and an evasive maneuver γ, h is a DT-ECBF on the set $\mathcal{C}$.*

Proof. Suppose $x \in \mathcal{C}$ so that $h(x) \geq 0$. Then

$$\Delta h(x, \gamma(x)) = \inf_{k \geq 1} \rho(\hat{x}_k) - \inf_{k \geq 0} \rho(\hat{x}_k).$$

The right hand side is nonnegative because it is the subtraction of the infimum of same function on different intervals where the first interval is a subset of the second interval. Then $\Delta h(x, \gamma(x)) \geq 0$. Recalling as well that $x \in \mathcal{C}$ means that $h(x) \geq 0$, this implies that $\Delta h(x, \gamma(x)) + \lambda h(x) \geq 0$. Then $\gamma(x) \in K(x)$ so h is a DT-ECBF. □

Remark 1. Although in Definition 1 $\mathcal{D}$ can be a larger set than $\mathcal{C}$, Theorem 1 is only valid for $\mathcal{C} = \mathcal{D}$. See [9] for sufficient conditions for $\mathcal{C} \subset \mathcal{D}$ in the continuous time domain.

3.2. The Effect of The Evasive Maneuver on Safe Sets

While Theorem 1 shows that h defined in (6) is a DT-ECBF and can therefore be used to guarantee safety, it does not explicitly imply anything about the topology of the safe set $\mathcal{C}$ that is implied by h. In particular, for different choices of γ, the associated safe set can be drastically different.

Consider the two examples given in [9] where the safety function is the distance between the two vehicles minus a safety distance, i.e.,

$$\rho(x(t)) = \sqrt{d_{1,2}(x)} - D_s. \tag{8}$$

An evasive maneuver where two vehicles turn at the same rate but have possibly different speeds is given by

$$\gamma_{turn} = \begin{bmatrix}\sigma v & \omega & 0 & v & \omega & 0\end{bmatrix}^T \tag{9}$$

where $0 < \sigma \leq 1$. A second evasive maneuver where two vehicles stay straight for all time is given by

$$\gamma_{straight} = \begin{bmatrix}v_1 & 0 & \zeta_1 & v_2 & 0 & \zeta_2\end{bmatrix}^T. \tag{10}$$

For notational convenience we denote h_{turn} and $h_{straight}$ as the h in (6) constructed from γ_{turn} and $\gamma_{straight}$, respectively. The reason these evasive maneuvers are considered in [9] is because they enable a closed form solution to (6) so that the barrier function constraint can be calculated in real-time. We consider some examples where the safe set implied by h_{turn} and $h_{straight}$ results in either an unnecessary invasive override or labeling states as unsafe that have ample room to avoid a collision. A graphical view of these two scenarios is in Figure 1. The actual path traversed by the vehicles for the scenario of Figure 1b is demonstrated in Figure 2.

Example 1. *States Are Labelled Unsafe Where Collisions Can Be Avoided.* Suppose h is parameterized by $\gamma_{straight}$ and consider an initial condition where the two vehicles are positioned at the same altitude with orientations pointing at each other. Then no matter how far apart the vehicles start, the calculation of (6) yields $h = -D_s$, implying that the initial conditions are not safe. This is because using $\gamma_{straight}$ as the evasive maneuver implies that the two vehicles will continue on a collision course until they collide. Clearly, as the vehicles are placed arbitrarily far apart, there is ample time to turn to avoid a collision. Nevertheless, according to $h_{straight}$, this configuration is outside of the safe set. Note that this scenario has been previously discussed in [14] where it was shown that there does not exist a finite range sensor to create a sensor compatible barrier function given $h_{straight}$.

Example 2. *An Unnecessary Invasive Override.* While using h_{turn} resolves the issue raised in Example 1, there are other initial conditions that lead to an unnecessary override even when using γ_{turn}. For instance, suppose that the vehicles pass on the left of each other with a lateral separation of more than the safety distance but less than four turn radii. Then if the vehicles continue straight the vehicles will eventually approach an unsafe condition according to h_{turn} and the overriding safety controller will induce a large path correction so that each vehicle can pass on the others' right.

Examples 1 and 2 indicate $h_{straight}$ and h_{turn} may be restrictive. Another way of looking at this problem is to plot the set of unsafe states for a variety of configurations as is done in Figure 3. Figure 3 demonstrates that even when the vehicles are not pointing at each other, the vehicles can be spaced far apart and be in an unsafe state when using $\gamma_{straight}$ as the evasive maneuver. Further, Figure 3a even shows that the vehicles can be considered unsafe even when they have flown past each other when using h_{turn}. The point of these examples is that there are cases where a barrier function can induce overly restrictive safety overrides. We note that while these two examples demonstrate that a safety override using barrier functions may result in overly restrictive behavior this is not necessarily the case for all barrier functions. In particular, this paper resolves these issues by finding a barrier function whose safe set is much larger than the safe set associated with either h_{turn} or $h_{straight}$ (see Fig. 5). It also shows using a maximum of barrier functions can increase the admissible control

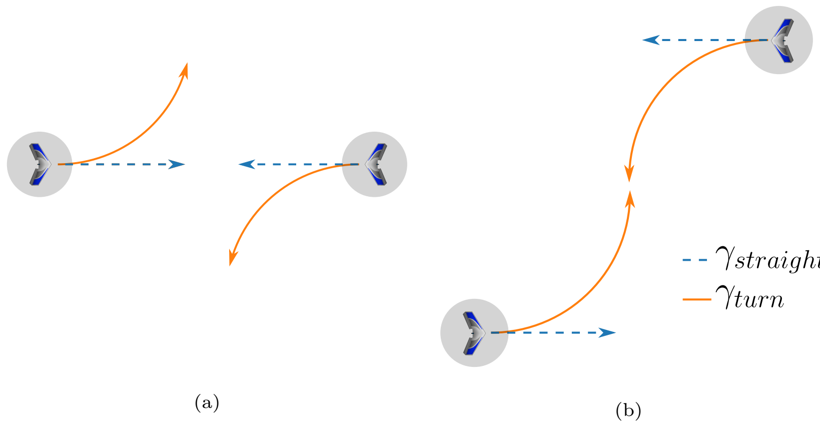

Figure 1: (a) When the two vehicles are pointing towards each other, the vehicles are not safe when using $h_{straight}$ no matter how far apart the vehicles start from each other. (b) When the vehicles pass to each others' left, the vehicles are not in the safe set when using h_{turn} because the evasive maneuver implies the vehicles would collide with each other. The practical takeaway in these two cases is that even though safety can be guaranteed, the particular states that are safe may be different. In either case though, collision avoidance can be achieved provided the vehicles start in a state such that $h(x) \geq 0$ for either $h_{straight}$ or h_{turn}.

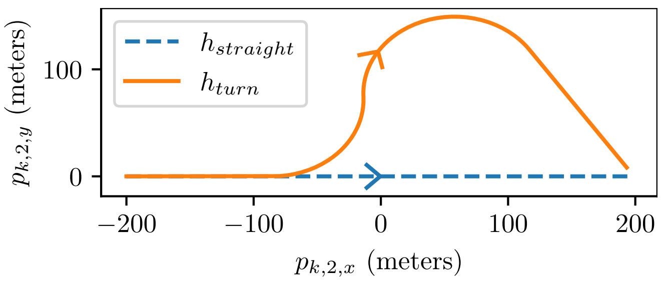

Figure 2: A plot of the trajectory of vehicle 2. When using $\gamma_{straight}$ to construct the barrier function, vehicle 2 does not deviate from the nominal control value. When using γ_{turn}, vehicle 2 deviates significantly. This is because the barrier function always makes sure that vehicle 2 can execute γ_{turn} to keep the vehicles safe even if there are better selections for an overriding controller (e.g., in this case, continuing straight). The trajectory for vehicle 1 is similar.

space.

3.3. An Initial Model Free Barrier Function

The issues in Figures 1 and 3 result because the evasive maneuvers used to calculate h are constant. More complicated evasive maneuvers might for instance involve turning right when the other vehicle is on the left and turning left when the other vehicle is on the right. More generally, we might expect that the evasive maneuver use the state to select an evasive maneuver which is not the case for $\gamma_{straight}$ and γ_{turn}. In this section we present a solution to this problem.

Another consideration not discussed in Section 3.2 for using Theorem 1 is that it requires that (6) be calculated over an infinite horizon. Nevertheless, as demonstrated in [9], h can be calculated in closed form for γ_{turn} and $\gamma_{straight}$. To do so, the authors of [9] assume a particular model and choose an evading maneuver to enable closed form calculations. However, as shown in Section 3.2, this may result in safe sets that exclude many seemingly safe states.

More generally, it may be difficult to generate a barrier function if the system dynamics are complicated. Nevertheless, as demonstrated in Theorem 1, the evasive maneuver can be any function that maps from the state to the action space.

Because it may be difficult to calculate h in (6) in closed form for an arbitrary γ, we propose taking a data driven approach. To do so, we can start the state at some $x_0 \in \mathbb{R}^n$ and apply some evasive maneuver γ that we specify.[2] Because the nominal controller is available, we could for instance let $\gamma = \hat{u}$ and create a sequence $\{x_k\}_{k=0}^{T}$ where T is some horizon over which safety is evaluated. In the case of UAV collision avoidance, T may represent battery life of the vehicles where collisions will obviously not occur beyond time T.

[2]Note that x_0 is sampled from $\mathbb{R}^n$ rather than $\mathcal{D}$ during the data-generation phase. This is to provide more data in fitting the learned $\hat{h}$. If the data did not include unsafe states then the data would have a bias towards predicting that states are safe.

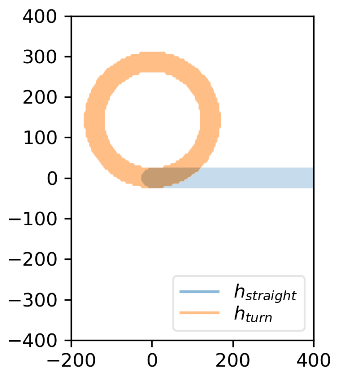

(a)

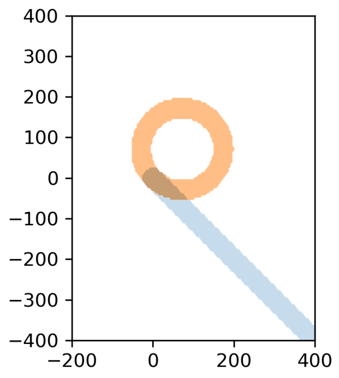

(b)

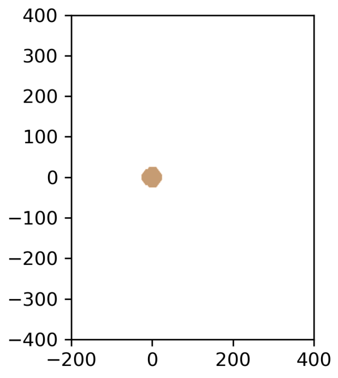

(c)

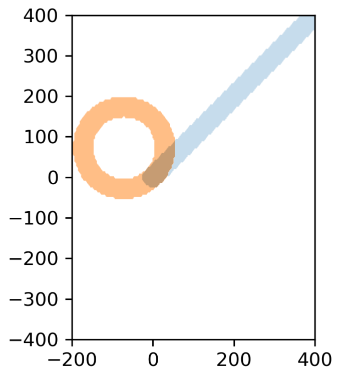

(d)

Figure 3: A plot of the unsafe set for four different configurations of the aircraft when using $h_{straight}$ (blue) or h_{turn} (orange). In all cases one of the vehicles is at the origin with orientation pointing along the positive x-axis. The plot shows when the set of states that are outside the safe set as the second vehicle changes x and y positions. In particular, it shows that some states are needlessly labelled unsafe. An example is in (a) where h_{turn} labels states as unsafe even when the vehicles have flown past each other. (a) The second vehicle is pointing left. (b) The second vehicle is pointing up. (c) The second vehicle is pointing right, (d) The second vehicle is pointing down.

Note that the sequence $\{x_k\}_{k=0}^{T}$ is the enumeration of the minimum on the right hand side of (6). Thus, given a starting state x_0, we can calculate $\rho_{min} = \min_{k \geq 0} \rho(x_k)$ to calculate a sample $h(x_0)$. Suppose this process is repeated N times to form a dataset $D = \{(x_0^j, \rho_{min}^j)\}_{j=1}^{N}$. Then we can fit a function $\hat{h}$ to approximate the mapping (6) with the dataset D. In the perfect case where there is no error in $\hat{h}$ we are left with a function that directly calculates (6) without having to do the integration in (6) because the integration is implicit in the fitting of the data.

However, when fitting $\hat{h}$ there will be errors. Errors where the learned $\hat{h}$ is less than the true h leads to more conservative behavior by considering states to be unsafe that are actually safe. On the other hand, when the learned $\hat{h}$ over predicts relative to the data, it can imply the state is safe when it is not. A conservative approach is to therefore bias the learned $\hat{h}$ downward to reflect uncertainty. This can be done by biasing the loss function as was done in [15] or alternatively with a Bayesian approach (e.g., Gaussian Processes [16] were used for barrier functions in [17]. Bayesian neural networks [18, 19] can also output an uncertainty) by subtracting a desired number of standard deviations from the model output. We note though that while this method reduces the chances that the fitted $\hat{h}$ will over predict the true h, because it cannot be guaranteed this type of error does not occur, the strict safety guarantee arising from Theorem 1 is lost.

3.4. Iteratively Expanding the Admissible Control Space

Consider the output of $\hat{h}$ when applied to fixed wing collision avoidance with a waypoint finding nominal controller. Position two vehicles arbitrarily far apart with waypoints located at the starting position of the other vehicle, and orientations pointing at their respective waypoint. This configuration will be unsafe for $\hat{h}$ for the same reason as described in Example 1. We now show how to improve on this initial estimated $\hat{h}$ with an iterative algorithm.

We therefore examine the case where a barrier function h is available and seek to generate a new barrier function h^1 with a larger safe set than h. Given a state $x_0 \in \mathbb{R}^n$ and a nominal control value $\hat{u}$, let $\gamma^1 : \mathbb{R}^n \to U$ be the result of the optimization[3] in equation (5). We note that the function γ^1 can be used as an evasive maneuver since it is a function that maps to the action space as required by Theorem 1. In other words, we can form a new barrier function h^1 via (6) such that

$$h^1(x_0) = \min_{k \geq 0} \rho(\hat{x}_k) \tag{11}$$

where

$$\hat{x}_{k+1} = f(\hat{x}_k, \gamma^1(\hat{x}_k)). \tag{12}$$

We denote the safe set of h^1 as $\mathcal{C}^1$.

Theorem 2. *Given a dynamical system (1) let h be defined in (6) with safety function ρ and evasive maneuver γ. Let h^1 be defined in (11) with safety function ρ and evasive maneuver γ^1 defined as the output of (5). Then $\mathcal{C} \subseteq \mathcal{C}^1$.*

Proof. Let $x_0 \in \mathcal{C}$. From Proposition 1, because γ^1 maps to values in $K(x)$ for all $x \in \mathcal{D}$, $\rho(\hat{x}_k) \geq 0$ for $k \geq 0$ where $\hat{x}_k$ is defined in (12). Then $h^1(x_0) \geq 0$. Then $x_0 \in \mathcal{C}^1$. $\square$

Theorem 2 says that by using γ^1 rather than γ as the evasive maneuver, the safe set does not get smaller. We now show a case where $\mathcal{C}$ is a strict subset of $\mathcal{C}^1$.

Example 3. Consider a discrete double integrator system

$$x_{k+1} = \begin{bmatrix} 1 & \Delta t \\ 0 & 1 \end{bmatrix} x_k + \begin{bmatrix} 0 \\ \Delta t \end{bmatrix} u, \tag{13}$$

where $x_{k,1}$ is the position and $x_{k,2}$ is the velocity. Let $\rho(x_k) = x_{k,1}$ so that the system is point wise safe when the position is nonnegative. Let $\gamma(x) = 1$ and $\Delta t = 0.1$. Let $x_0 = \begin{bmatrix} 0.5 & -1 \end{bmatrix}^T$. Then $h(x_0) = -0.05$ so $x \notin \mathcal{C}$. In the case

[3]Note that because x_0 is sampled from $\mathbb{R}^n$ rather than $\mathcal{D}$ it is not guaranteed that the optimization program has a solution when $x \notin \mathcal{D}$. This can be resolved for instance by adding a slack variable.

where $\hat{u} = 2 \in U$, the result of (5) is $\gamma^1(x) = 2$. Then using γ^1 to construct h^1 via (11), $h^1(x_0) = 0.2$ so $x_0 \in \mathcal{C}^1$.

The point of Example 3 is that γ^1 can in some cases do a better job at avoiding unsafe conditions and as a result the safety set is enlarged. However, as discussed in Section 3.3, there is a drawback to using γ^1. In particular, to apply Theorem 2, one then needs to forward propagate the dynamics (12) for all future time where the controller at every future timestep is the result of a nonconvex program (5) and return the minimum $\rho(x_k)$ for the resulting sequence $\{\hat{x}_k\}_{k=0}^T$. For online safety overrides, this is not computationally feasible. Thus, we pursue the data driven approach discussed in Section 3.3. The algorithm is described in Algorithm 1.

Given Theorem 2 and Example 3 and that there are no errors in fitting $\hat{h}^1$ to to h^1, we expect that $\mathcal{C}^1$ will be a superset of $\mathcal{C}$. However, notice that we can continue this process to form γ^2 with the property that $\gamma^2(x) \in K^1(x)$ for all $x \in \mathcal{C}^1$ where

$$K^1(x) = \{u \in U \ : \ \Delta\hat{h}^1(x) + \gamma\hat{h}^1(x) \geq 0\}. \tag{14}$$

This approach is summarized in Algorithm 2. In general, for a barrier function h^i we denote the admissible control space by K^i and the safe set by $\mathcal{C}^i$.

However, Algorithm 2 ignores a subtle issue, namely that it is not necessarily the case that $K^j(x) \subseteq K^i(x)$ for any $i > j$ even though Theorem 2 shows that $\mathcal{C}^j \subseteq \mathcal{C}^i$. This is demonstrated in the following example.

Example 4. Consider again the double integrator system in Example 3. Let $x_0 = \begin{bmatrix} 2 & -1 \end{bmatrix}$, $\gamma(x) = 0.5$, and $\lambda = 0.9$. Then a numerical calculation shows that $K(x_0) = \{u \ : \ u \geq -3.77\}$. Let

$$\hat{u}(x) = \begin{cases} 1 & x_{0,0} = 2 \text{ and } x_{0,1} = -1 \\ 0.5 & \text{otherwise} \end{cases}.$$

Then $K^1(x_0) = \{u \ : \ u \geq -3.67\}$. In other words, even though Theorem 2 shows that $\mathcal{C} \subseteq \mathcal{C}^1$, it is not the case that $K(x) \subseteq K^1(x)$.

Algorithm 1: Initial algorithm for learning a model free barrier function.

```
input  : $h$ (barrier function), $N$ (number of samples), $\hat{u}$ (nominal
         controller), $T$ (safety horizon)
output: $\hat{h}^1$
1  Function ExpandSafeSet($h$, $\rho$, $N$, $T$):
2      $D = \{\}$;
3      for $m \leftarrow 1$ to $N$ do
4          select a random $x_0$;
5          $x \leftarrow x_0$;
6          $\rho_{min} \leftarrow \rho(x)$;
7          for $j \leftarrow 1$ to $T$ do
8              $\gamma^1 \leftarrow$ from equation (5) using $x$, $h$, and $\hat{u}$;
9              $x \leftarrow f(x, \gamma^1)$;
10             $\rho_{min} \leftarrow \min(\rho_{min}, \rho(x))$;
11         end
12         append $\{x_0, \rho_{min}\}$ to $D$;
13     end
14     $\hat{h}^1 \leftarrow$fit to $D$;
15     return $\hat{h}^1$;
```

Algorithm 2: Algorithm for Iteratively Expanding the Safe Set

```
input  : $h$ (barrier function), $N$ (number of samples), $\hat{u}$ (nominal
         controller), $T$ (safety horizon), $L$ (number of expansions)
output: $\hat{h}^L$
1  $\hat{h}^0 \leftarrow h$;
2  for $i \leftarrow 1$ to $L$ do
3      $\hat{h}^i \leftarrow$ExpandSafeSet($\hat{h}^{i-1}$, $\rho$, $N$, $\hat{u}$, $T$);
4  end
```

Example 4 shows that even though the safe set is enlarged when using Algorithm 2, the set of controls available to keep the system safe may be reduced. This means that in some places of the safe set there may be a more aggressive safety override when using h^1 rather than h. For this reason we would like to use the maximum of the barrier functions h^j for $j \leq i$ in Algorithm 2. We note that the use of maximums for boolean composition of barrier functions for continuous time systems was previously analyzed in [20].

Theorem 3. *Given a dynamical system (1) and DT-ECBFs h^1 and h^2, the function h^3 defined by $h^3(x) = \max(h^1(x), h^2(x))$ is a DT-ECBF on the set $\mathcal{C}^1 \cup \mathcal{C}^2$. Further, $K^1(x) \subseteq K^3(x)$ on the set $\mathcal{C}^1$ and $K^2(x) \subseteq K^3(x)$ on the set $\mathcal{C}^2$.*

Proof. We first prove that h^3 is a DT-ECBF on $\mathcal{C}^1 \cup \mathcal{C}^2$. Suppose $x \in \mathcal{C}^1 \cup \mathcal{C}^2$ and without loss of generality, assume $h^1(x) \geq h^2(x)$ so $h^3(x) = h^1(x)$. Suppose $u \in U$ satisfies $\Delta h^1(x,u) + \lambda h^1(x) \geq 0$ and let $x_1 = f(x,u)$. Such a u exists because h^1 is a DT-ECBF. Then

$$\begin{aligned} &\Delta h^3(x,u) + \lambda h^3(x) \\ &\quad = [\max(h^1(x_1), h^2(x_1)) - \max(h^1(x), h^2(x))] + \lambda \max(h^1(x), h^2(x)) \\ &\quad = \max(h^1(x_1), h^2(x_1)) - h^1(x) + \lambda h^1(x). \end{aligned} \tag{15}$$

Case 1: If $h^1(x_1) \geq h^2(x_1)$ then (15) becomes

$$\Delta h^3(x,u) + \lambda h^3(x) = \Delta h^1(x,u) + \lambda h^1(x) \geq 0.$$

Case 2: If $h^1(x_1) < h^2(x_1)$ then (15) becomes

$$\begin{aligned} \Delta h^3(x,u) + \lambda h^3(x) &= h^2(x_1) - h^1(x) + \lambda h^1(x) \\ &\geq h^1(x_1) - h^1(x) + \lambda h^1(x) \\ &= \Delta h^1(x,u) + \lambda h^1(x) \geq 0. \end{aligned}$$

Then h^3 is a DT-ECBF.

Note that this also establishes that $K^1(x) \subseteq K^3(x)$ on the set $\mathcal{C}^1$ under the condition that $h^1(x) \geq h^2(x)$. We now consider the case where $x \in \mathcal{C}^1$ and

$h^1(x) < h^2(x)$ to show that $K^1(x) \subseteq K^3(x)$ on the set $\mathcal{C}^1$. When $h^1(x) < h^2(x)$ we have

$$\begin{aligned}
&\Delta h^3(x,u) + \lambda h^3(x) \\
&\quad = [\max(h^1(x_1), h^2(x_1))] - h^2(x) + \lambda h^2(x) \\
&\quad \geq [\max(h^1(x_1), h^2(x_1))] - h^1(x) + \lambda h^1(x).
\end{aligned}$$

Continuing the same logic as cases 1 and 2 above we conclude $K^1(x) \subseteq K^3(x)$ on the set $\mathcal{C}^1$ under the condition that $h^1(x) < h^2(x)$. Then $K^1(x) \subseteq K^2(x)$ on $\mathcal{C}^1$. The case of $K^2(x) \subseteq K^3(x)$ on $\mathcal{C}^2$ is proven the same way. □

Remark 2. The optimization (5) is non-convex so finding an online solution may be computationally intensive. A direct solution to this is to assume U is a small finite set and allow the calculation to be done in a single forward pass of a neural network. However, an alternative occurs when h^1 is defined via (6) for some γ and $x \in \mathcal{C}^1$. Theorem 1 demonstrates that γ is always a feasible solution of (5) provided $h^1(x) \geq 0$ (and similarly for an evasive maneuver used to construct h^2 for $x \in \mathcal{C}^2$). Because $K^1(x) \subseteq K^3(x)$ for all $x \in \mathcal{C}^1$, this means that γ is a feasible solution for (5) when using h^3 and $x \in \mathcal{C}^1$.

Theorem 3 provides the justification for adjusting Algorithm 2 to use a maximum so that the safety set is enlarged as well as the admissible control space. However, the direct application of Theorem 3 implies that L barrier functions must be maintained, which implies memory growth and reduces online computation capability. For this reason, we elect to adjust the dataset accordingly in Algorithm 3. Note that the difference between the functions ExpandSafeSet and ExpandSafeSetWithMax occurs in line 17 in Algorithm 3 where the max is used.

3.5. Model Free Barrier Functions

While h^L in Algorithm 3 may appear to be model-free, a model is still required to select $\gamma^1(x)$ in line 12 because $K(x)$ requires a calculation of $\Delta h(x,u)$ which requires a model for the dynamics. Thus, to make the final result of

Algorithm 3: Algorithm for Iteratively Expanding the Safe Set and the Admissible Control Space

```
   input  : $h$ (barrier function), $N$ (number of samples), $\hat{u}$ (nominal
            controller), $T$ (safety horizon), $L$ (number of expansions)
   output: $\hat{h}^L$
1  $\hat{h}^0 \leftarrow h$;
2  for $i \leftarrow 1$ to $L$ do
3      $\hat{h}^i \leftarrow$ExpandSafeSetWithMax($h^{i-1}$, $\rho$, $N$, $T$);
4  end
5  Function ExpandSafeSetWithMax($h$, $\rho$, $N$, $\hat{u}$, $T$):
6      $D = \{\}$;
7      for $m \leftarrow 1$ to $N$ do
8          select a random $x_0$;
9          $x \leftarrow x_0$;
10         $\rho_{min} \leftarrow \rho(x)$;
11         for $j \leftarrow 1$ to $T$ do
12             $\gamma^1 \leftarrow$ from equation (5) using $x$, $h$, and $\hat{u}$;
13             $x \leftarrow f(x, \gamma^1)$ ;
14             $\rho_{min} \leftarrow \min(\rho_{min}, \rho(x))$;
15         end
16     end
17     append $\{x_0, \max(h(x_0), \rho_{min})\}$ to $D$;
18     $\hat{h}^1 \leftarrow$fit to $D$;
19     return $\hat{h}^1$;
```

Algorithm 3 model-free we must also create a learned function $\Delta\hat{h}$. To do so, we simply record the minimum $\rho(x)$ occurring after $j = 1$ in Algorithm 3.

4. SIMULATION EXPERIMENTS

In this section we validate the approach of Algorithm 3. We let $v_1 = v_2 = 15$ meters/second in equation (10) and restrict the action space of both agents to a selection of $[-12, 0, 12]$ degrees per second for ω while holding velocity fixed at 15 meters per second and altitude rate at 0. The initial state for each vehicle is between $\begin{bmatrix}-200 & -200 & -\pi & 0\end{bmatrix}^T$ and $\begin{bmatrix}200 & 200 & \pi & 0\end{bmatrix}^T$. We also let $\rho(x) = \max(50, \sqrt{d_{1,2}(x)} - D_s)$. We use a ρ that is clipped at 50 rather than just $\sqrt{d_{1,2}(x)} - D_s$ to simplify data normalization so that the target values are not unbounded and note that this clipping does not change $\mathcal{C}$. Hyperparameters are listed in Table 1 and training statistics are plotted in Figure 4.

Similar to Figure 3, we plot in Figure 5 the safe set for the mean value of the model free barrier function as well as when three standard deviations are subtracted. When subtracting three standard deviations from the mean output of the model-free barrier function, the unsafe set is enlarged. We also plot how the unsafe set changes as the ExpandWithMax in Figure 6 to demonstrate that the safe set is enlarged as the algorithm proceeds.

We list the percentage of collisions at each training iteration in Table 2. Given the model-free barrier function at the given iteration we show what percentage of episodes the vehicles come within 25 meters of each other when the barrier function value of the first state is nonnegative. Notice that the number of collisions when using a model free barrier function is less than 10% of the number of collisions when using no barrier function. Additionally note that there are not zero collisions when using a model-free barrier function as there is noise in fitting to the data. Nevertheless, safety is significantly improved over using the nominal controller alone.

Table 1: Hyperparameters when fitting a model free barrier function

Hyperparameter	Value
Learning Rate	1e-4
Batch Size	50000
Epochs	10000
Dropout Percent	50%
Num Samples for Stdev Calculation	50
Number of Fully Connected Layers	4
Width Per Layer	1024

Table 2: The percentage of episodes where the vehicles collide from random initial conditions when the initial state is safe according to the barrier function versus the scenario where only the nominal controller is used. Notice that safety is significantly improved when using a model-based barrier function but that safety is nevertheless not guaranteed as there is noise in fitting to the data.

Iteration	Barrier	No Barrier
1	0.2	8.9
2	0.5	8.8
3	0.4	8.9
4	0.5	8.8
5	0.5	9.0

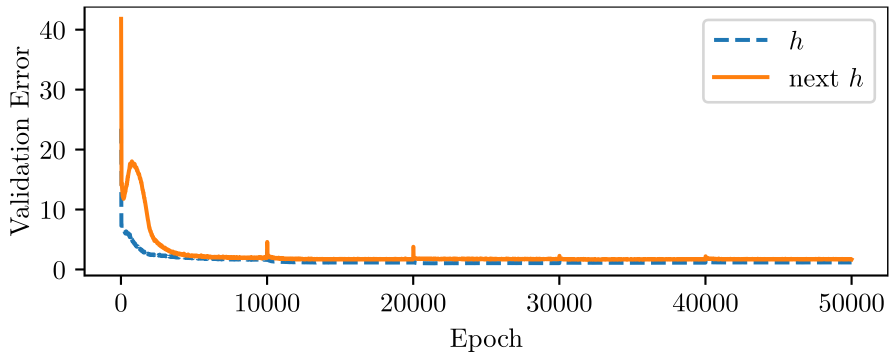

(a)

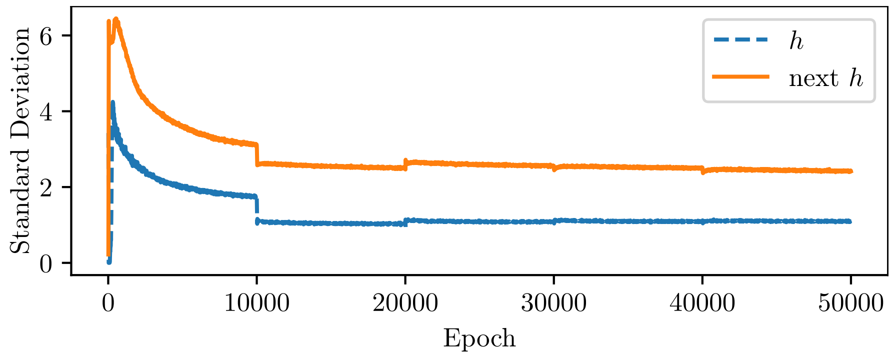

(b)

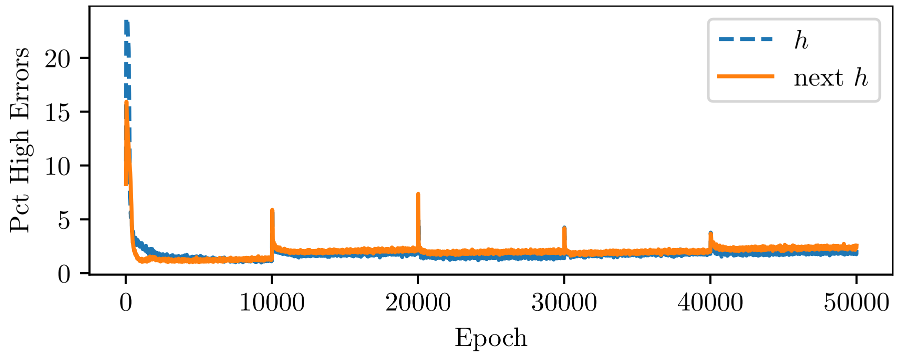

(c)

Figure 4: Training data when fitting a model-free barrier function. (a) The validation error of the model-free network, (b) The standard deviation output by the network, and (c) How often the network outputs a value that is higher than the true value when subtracting 3 standard deviations from the mean of the network output.

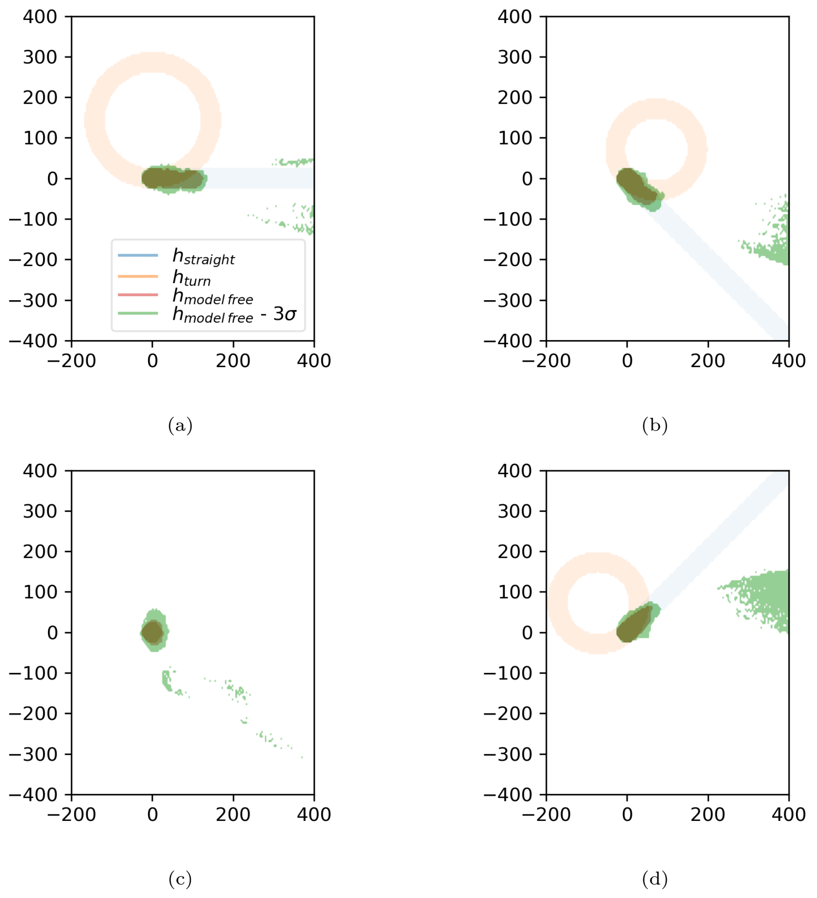

Figure 5: A plot of the unsafe set for the four different configurations of Fig. 3 for model based and a model free method. The model free method shows the mean output of a neural network as well as the case where we subtract three standard deviations from the mean. Note that the safe set for the mean output of the model free-barrier function is a subset of the model free unsafe sets. When subtracting 3 standard deviations from the model-free barrier function the unsafe set is larger than when using the mean. The data for fitting the model-free barrier function was sampled from positions (-200, -200) to (200, 200) so out-of-sample points are often labelled as unsafe due to the higher data uncertainty of those states. (a) The second vehicle is pointing left. (b) The second vehicle is pointing up. (c) The second vehicle is pointing right, (d) The second vehicle is pointing down.

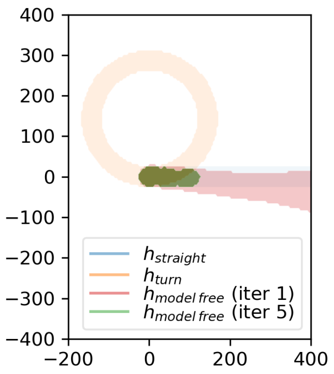

(a)

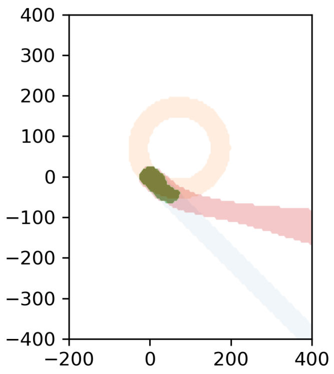

(b)

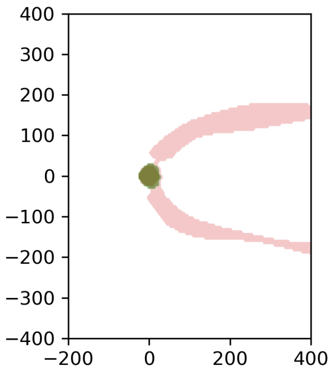

(c)

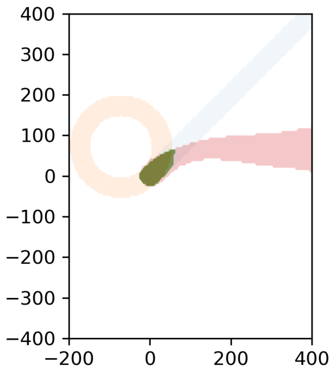

(d)

Figure 6: A plot of the unsafe set for the four different configurations of Fig. 3 for comparing early vs later iterations of the model free barrier functions. A plot demonstrating that the safe set grows as the algorithm proceeds. Note that on unsafe set of the barrier function at iteration 5 is a subset of the unsafe set at iteration 1, as predicted by Theorem 3. (a) The second vehicle is pointing left. (b) The second vehicle is pointing up. (c) The second vehicle is pointing right, (d) The second vehicle is pointing down.

5. CONCLUSION

In this paper we have discussed a few issues with model based barrier functions, namely that barrier functions may label safe states as unsafe (Example 1), barrier functions may cause unnecessary overrides that cause the state to get closer to the boundary of the safe set than without an override (Example 2), for complex systems it may be difficult to solve for a barrier function in closed form (h_{turn} and $h_{straight}$ exist due to closed form solutions but lead to large unsafe sets, see Fig. 5), and it can be numerically infeasible to solve for a barrier function when there is a long horizon (see equation (6)). To resolve these problems, we introduced model-free barrier functions which take a data-driven approach to developing a barrier function. The tradeoff is that because the barrier function cannot perfectly fit to the data, safety guarantees are lost but the benefit is that the safety set may be significantly enlarged (Fig. 5). Further, the optimization required to solve for a safe control input can be done in a single forward pass through a neural network. We demonstrated the efficacy of the approach in a fixed-wing aircraft collision avoidance scenario where, because of the model free barrier function, the safety of the system is significantly improved over using a nominal controller alone.

Declaration of competing interest

The authors declare that they have no known competing financial interests or personal relationships that could have appeared to influence the work reported in this paper.

Acknowledgements

This work was enabled by The National Science Foundation, Grant No. 1836932 and well as the University System of Georgia Tuition Assistance Program.

References

References

[1] A. D. Ames, X. Xu, J. W. Grizzle, P. Tabuada, Control barrier function based quadratic programs for safety critical systems, IEEE Transactions on Automatic Control 62 (8) (2017) 3861–3876. doi:10.1109/TAC.2016.2638961.

[2] L. Wang, D. Han, M. Egerstedt, Permissive barrier certificates for safe stabilization using sum-of-squares, in: 2018 Annual American Control Conference (ACC), 2018, pp. 585–590. doi:10.23919/ACC.2018.8431617.

[3] Z. Qin, K. Zhang, Y. Chen, J. Chen, C. Fan, Learning safe multi-agent control with decentralized neural barrier certificates, arXiv preprint arXiv:2101.05436.

[4] A. Robey, H. Hu, L. Lindemann, H. Zhang, D. V. Dimarogonas, S. Tu, N. Matni, Learning control barrier functions from expert demonstrations, in: 2020 59th IEEE Conference on Decision and Control (CDC), 2020, pp. 3717–3724. doi:10.1109/CDC42340.2020.9303785.

[5] R. Cheng, G. Orosz, R. M. Murray, J. W. Burdick, End-to-end safe reinforcement learning through barrier functions for safety-critical continuous control tasks, Proceedings of the AAAI Conference on Artificial Intelligence 33 (01) (2019) 3387–3395. doi:10.1609/aaai.v33i01.33013387.

[6] H. Ma, J. Chen, S. E. Li, Z. Lin, Y. Guan, Y. Ren, S. Zheng, Model-based constrained reinforcement learning using generalized control barrier function, arXiv preprint arXiv:2103.01556.

[7] U. Borrmann, L. Wang, A. D. Ames, M. Egerstedt, Control barrier certificates for safe swarm behavior, IFAC-PapersOnLine 48 (27) (2015) 68–73. doi:https://doi.org/10.1016/j.ifacol.2015.11.154.

[8] A. Nagabandi, G. Kahn, R. S. Fearing, S. Levine, Neural network dynamics for model-based deep reinforcement learning with model-free fine-tuning, in: 2018 IEEE International Conference on Robotics and Automation (ICRA), 2018, pp. 7559–7566. doi:10.1109/ICRA.2018.8463189.

[9] E. Squires, P. Pierpaoli, R. Konda, S. Coogan, M. Egerstedt, Composition of multiple safety constraints with applications to decentralized fixed-wing collision avoidance, arXiv preprint.

[10] E. Squires, Model free barrier functions via implicit evading maneuvers, https://youtu.be/QNbKrhUxPjk, accessed: 2021-07-21 (2021).

[11] A. Agrawal, K. Sreenath, Discrete control barrier functions for safety-critical control of discrete systems with application to bipedal robot navigation, in: Proceedings of Robotics: Science and Systems, Cambridge, Massachusetts, 2017, pp. 73–82. doi:10.15607/RSS.2017.XIII.073.

[12] J. Foerster, G. Farquhar, T. Afouras, N. Nardelli, S. Whiteson, Counterfactual multi-agent policy gradients, Proceedings of the AAAI Conference on Artificial Intelligence 32 (1).

[13] T. Gurriet, M. Mote, A. D. Ames, E. Feron, An online approach to active set invariance, in: 2018 IEEE Conference on Decision and Control (CDC), 2018, pp. 3592–3599. doi:10.1109/CDC.2018.8619139.

[14] E. Squires, R. Konda, P. Pierpaoli, S. Coogan, M. Egerstedt, Safety with limited range sensing constraints for fixed wing aircraft, in: 2021 International Conference on Robotics and Automation (ICRA) (to appear), IEEE, 2021.

[15] M. Srinivasan, A. Dabholkar, S. Coogan, P. A. Vela, Synthesis of control barrier functions using a supervised machine learning approach, in: 2020 IEEE/RSJ International Conference on Intelligent Robots and Systems (IROS), 2020, pp. 7139–7145. doi:10.1109/IROS45743.2020.9341190.

[16] C. E. Rasmussen, C. K. Williams, Gaussian processes for machine learning, Vol. 1, MIT press Cambridge, 2006.

[17] L. Wang, E. A. Theodorou, M. Egerstedt, Safe learning of quadrotor dynamics using barrier certificates, in: 2018 IEEE International Conference on Robotics and Automation (ICRA), 2018, pp. 2460–2465. doi:10.1109/ICRA.2018.8460471.

[18] C. Blundell, J. Cornebise, K. Kavukcuoglu, D. Wierstra, Weight uncertainty in neural network, in: F. Bach, D. Blei (Eds.), Proceedings of the 32nd International Conference on Machine Learning, Vol. 37 of Proceedings of Machine Learning Research, PMLR, Lille, France, 2015, pp. 1613–1622.

[19] Y. Gal, Uncertainty in deep learning, University of Cambridge 1 (3).

[20] P. Glotfelter, J. Cortés, M. Egerstedt, Nonsmooth barrier functions with applications to multi-robot systems, IEEE Control Systems Letters 1 (2) (2017) 310–315. doi:10.1109/LCSYS.2017.2710943.